

Tuning Magnetotransport through a Magnetic Kink Crystal in a Chiral Helimagnet

Jun-ichiro Kishine

Department of Basic Sciences, Kyushu Institute of Technology, Kitakyushu, 804-8550, Japan

I. V. Proskurin and A. S. Ovchinnikov

Department of Physics, Ural State University, Ekaterinburg, 620083, Russia

(Received 3 April 2011; published 1 July 2011)

We consider magnetotransport properties in a conducting chiral helimagnet, where the magnetic kink crystal (MKC) is formed under weak magnetic field applied perpendicular to the helical axis. The MKC behaves as a magnetic superlattice potential and results in Bragg scattering of conduction electrons. Tuning of the weak magnetic field enables us to control the size of the superlattice Brillouin zone and gives rise to a series of divergent resistivity anomalies originating from resonant Bragg scatterings. We discuss as well a nontrivial magnetic structure in the resonant states realized in the subsystem of the itinerant electrons.

DOI: 10.1103/PhysRevLett.107.017205

PACS numbers: 75.30.-m, 75.47.-m, 85.75.Ss

A coupling of free electrons with nontrivial spin textures has recently attracted a great deal of attention because of an ability to manipulate magnetotransport properties through control of the background spin subsystem. The central issues there include the current-driven motion of the magnetic domain wall (DW) and vortices [1], electromotive force generation [2], or magnetoresistance phenomena [3]. To explain the resistance change when the current flows through the magnetic texture, several theoretical ideas have been proposed: mixing of spin states due to the background magnetic texture [4], destruction of the weak localization by the DW [5], spin accumulation around the DW [6], appearance of the texture-dependent resistivity tensor due to dissipative spin-motive force generated by magnetization dynamics [7]. It is, however, still under debate whether the domain wall resistivity is positive or negative [8].

The aim of this Letter is to address a complementary mechanism of magnetoresistance for electrons traveling through a magnetic superlattice structure stabilized in a chiral helimagnet. In chiral helimagnet, the left- or right-handed helical spin texture along the crystallographic axis is stabilized by a competition between symmetric J and antisymmetric Dzyaloshinskii-Moriya (DM) exchange interactions [9,10] specified by the DM vector $\mathbf{D} = D\hat{\mathbf{e}}_z$ along the helical axis. The helical pitch, $L_0 = 2\pi/Q_0$, is fixed by $Q_0 = a_0^{-1}\tan^{-1}(D/J)$. a_0 is the lattice unit of the constituent crystallographic cubic lattice.

Under a weak magnetic field applied perpendicular to the helical axis, $\tilde{H} = 2\mu_B H\hat{\mathbf{e}}_x$ (μ_B is the Bohr magneton and H is a strength of the field), the ground state forms a magnetic superlattice called a magnetic kink crystal (MKC) or sometimes referred to as a chiral soliton lattice [11,12] as shown in Fig. 1(a). Previously, we have studied magnetic current carried by a sliding motion of the MKC [13], a novel spin resonance associated with the MKC elementary excitations [14], and a current-driven sliding

motion of the MKC [15]. The MKC state is described by the semiclassical spin vector, $\mathbf{S}_i = S\mathbf{n}(z_i) = S(\cos\varphi(z_i), \sin\varphi(z_i), 0)$ with the winding angle being given by $\cos(\varphi(z)/2) = \text{sn}(2Kz/L_{\text{MKC}})$. Here, sn is the Jacobi elliptic function with the elliptic modulus κ ($0 \leq \kappa < 1$), K and E are the complete elliptic integrals of the first and second kind. The spatial period of the MKC superlattice is given by $L_{\text{MKC}} = 8KE/(\pi Q_0)$ which continuously increases from L_0 to infinity when the magnetic field increases from zero to the critical strength $\tilde{H}_c = (\pi Q_0 a_0/4)^2 JS \sim D^2/J$. In practice, the critical field is of the order of 100–1000 G [16]. The elliptic modulus κ is determined from the condition of the minimal energy per the period $\tilde{H}/\tilde{H}_c = (\kappa/E)^2$.

Now, let us consider a conducting chiral helimagnet, where free electrons with the hopping integral t are coupled with the background MKC texture via the sd-type interaction of the strength J_{sd} . A possible experimental candidate of such a system is currently available, $\text{Cr}_{1/3}\text{NbS}_2$ [17]. To be more precise, we specify a hierarchy of the relevant energy scales for the itinerant electron subsystem as $\tilde{H}_c \ll J_{\text{sd}} \ll t$. The condition enables us to neglect an orbital bending and a Zeeman coupling of the conduction electrons due to the external magnetic field. As a consequence, relevant magnetic effects discussed below originate from the sd coupling and an inner gauge field of order t , as discussed below. Under these assumptions, the itinerant electrons feel periodic potentials associated with both the host atomic lattice and the magnetic superlattice formed by the MKC state. Therefore, there are two independent reciprocal lattice scales associated with atomic lattice, $G_0 = 2\pi/a_0$, and the MKC superlattice,

$$G_{\text{MKC}} = 2\pi/L_{\text{MKC}}. \quad (1)$$

Since $a_0 \ll 2\pi/Q_0 \leq L_{\text{MKC}}$ one sees that $G_{\text{MKC}} \ll G_0$ and the superlattice Brillouin zone (BZ) is much narrower

than the atomic BZ. We here emphasize that the size of the superlattice can be controlled by the magnetic field. Then, a natural question arises whether the magnetic superlattice BZ affects electron conduction, or, to be precise, is whether a band insulator state emerges due to umklapp scattering related with G_{MKC} . In this Letter, we present a study of this issue.

In what follows, we assume that an electric field is applied along the helical axis, and dc electric current flows along the same direction. Being the MKC state given as a rigid background superlattice, we take the Hamiltonian for electrons interacting with the superlattice via the sd interaction in the form $\mathcal{H} = \mathcal{H}_{\text{el}} + \mathcal{H}_{\text{sd}}$, where the free electron part is

$$\mathcal{H}_{\text{el}} = -t \sum_{(i,j),\sigma} \hat{c}_{i,\sigma}^\dagger \hat{c}_{j,\sigma} - \mu \sum_{i,\sigma} \hat{c}_{i,\sigma}^\dagger \hat{c}_{i,\sigma}. \quad (2)$$

Here, i and j are the nearest neighbor sites, $\hat{c}_{i,\sigma}^\dagger$ ($\hat{c}_{i,\sigma}$) represents a creation (annihilation) operator for the electron with spin projection σ at the i th site, and μ is the chemical potential. The sd term is

$$\mathcal{H}_{\text{sd}} = -J_{\text{sd}} \sum_i \mathbf{S}_i \cdot \hat{\mathbf{s}}_i, \quad (3)$$

where $\hat{\mathbf{s}}_i = (1/2)\hat{c}_{i\alpha}^\dagger \boldsymbol{\sigma}_{\alpha\beta} \hat{c}_{i\beta}$ represents quantum spin $1/2$, $\boldsymbol{\sigma}$ are the Pauli's matrices. In the representation, the electron spin quantization axis coincides with the crystallographic z axis.

The next step is to decompose a process embedded in \mathcal{H} into diagonalized quasiparticle and scattering counterparts. For this purpose, we rotate the spin quantization axis to the direction of the local spin \mathbf{S}_i by using the local SU(2) gauge transformation, $\hat{c}_i = \hat{U}_i \hat{b}_i$, where $\hat{U}_i = \exp[\frac{i}{2} \boldsymbol{\alpha}(z_i) \cdot \boldsymbol{\sigma}]$. The rotation vector is given by $\boldsymbol{\alpha}(z) = \frac{\pi}{2}(-\sin\varphi(z), \cos\varphi(z), 0)$. The geometrical picture is as follows. The vector $\boldsymbol{\alpha}(z)$ points to the direction of $\hat{\mathbf{e}}_z \times \mathbf{n}(z)$. Then, $\pi/2$ rotation around $\hat{\boldsymbol{\alpha}}$ makes the local quantization axis parallel to the direction of $\mathbf{n}(z)$. Consequently, the crystal frame xyz is transformed into the local frame $\bar{x}\bar{y}\bar{z}$, where the sd term is diagonalized as $\mathbf{S}_i \cdot \hat{\mathbf{s}}_i = (S/2)\hat{b}_i^\dagger \sigma^z \hat{b}_i$. The cost of diagonalizing the sd term is the appearance of the gauge field coming from the hopping term, $-t\hat{c}_{i,\sigma}^\dagger \hat{c}_{i+1,\sigma} = -t\hat{b}_i^\dagger \hat{U}_i^\dagger \hat{U}_{i+1} \hat{b}_{i+1}$, where $\hat{b}_i^\dagger = (\hat{b}_{i1}^\dagger, \hat{b}_{i2}^\dagger)$. Because we consider the slowly varying spin texture, the gradient expansion with respect to small $a_0 \partial_z \varphi(z)$ is legitimate. Then, we have $\hat{U}_i^\dagger \hat{U}_{i+1} \approx 1 + a_0 \hat{U}^\dagger \partial_z \hat{U} = 1 + i\mathbf{A}(z_i) \cdot \boldsymbol{\sigma}$, where the gauge field is introduced by

$$\mathbf{A}(z) = \frac{a_0}{2} \partial_z \varphi(z) (-\cos\varphi(z), -\sin\varphi(z), 1), \quad (4)$$

which has a period L_{MKC} .

Consequently, the Hamiltonian is reorganized as $\mathcal{H} = \mathcal{H}_{\text{el}} + \mathcal{H}_{\text{sd}} = \mathcal{H}_{\text{QP}} + \mathcal{H}_{\text{scatt}}$. The quasiparticle term is given in the Fourier transformed form as

$\mathcal{H}_{\text{QP}} = \sum_{k,\sigma} \varepsilon_{k,\sigma} \hat{b}_{k,\sigma}^\dagger \hat{b}_{k,\sigma}$ with the spectrum being given by $\varepsilon_{k,\sigma} = -2t \cos(ka_0) - \mu - h_{\text{sd}} \sigma$, where the effective field ("sd field") $h_{\text{sd}} = SJ_{\text{sd}}/2$ acts on the quasiparticles. The $\sigma = \pm 1$ represents the projection of spin on the local quantization axis. The gauge field term gives rise to the scattering term given by $\mathcal{H}_{\text{scatt}} = -it \sum_i \hat{b}_i^\dagger [\mathbf{A}(z_i) \cdot \boldsymbol{\sigma}] \hat{b}_{i+1} + \text{c.c.}$ In Fig. 1(b), we depict the coupling of the free electrons with the diagonalized sd-field part H_{sd} , and the nondiagonalized gauge field potential in the local frame $\bar{x}\bar{y}\bar{z}$. The sd field causes the band splitting into the spin up and down bands, as shown in Fig. 1(c).

By introducing the Fourier transform, $\mathbf{A}_q = L^{-1} \sum_i e^{-iqz_i} \mathbf{A}(z_i)$, where L is a linear size of the system, the scattering term takes the form

$$\mathcal{H}_{\text{scatt}} = 2t \sum_{k,q} e^{-iq a_0/2} \sin(ka_0) \hat{b}_{k+q/2}^\dagger (\mathbf{A}_q \cdot \boldsymbol{\sigma}) \hat{b}_{k-q/2}, \quad (5)$$

which fully describes the scattering processes of the quasiparticles.

From $\mathbf{A} \cdot \boldsymbol{\sigma} = (A^+ \sigma^- + A^- \sigma^+)/2 + A^3 \sigma^3$ with $A^\pm = A^1 \pm iA^2$ it follows that the gauge field acts as a periodic vector potential that provides both spin-conserving (A^3) and spin-flipping (A^\pm) scatterings of electrons. As a consequence, the scattering term (5) causes an elastic umklapp scattering process with a series of special wave numbers

$$q = q_n = nG_{\text{MKC}}, \quad (6)$$

(n is a nonzero integer) under the condition of energy conservation,

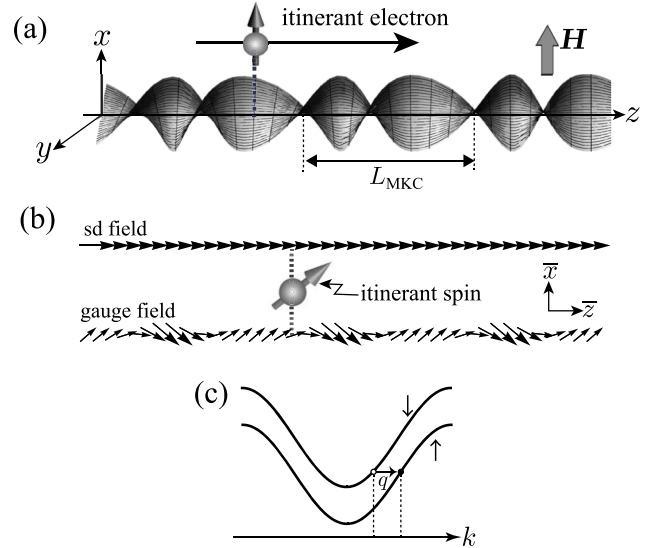


FIG. 1 (color online). (a) Magnetic kink crystal (MKC) state coupled with itinerant spins via the sd coupling. The magnetic field strength must satisfy the weak field condition ($\omega_c \tau_{\text{el}} \ll 1$), where ω_c is the cyclotron resonance frequency and τ_{el} is the Boltzmann relaxation time of the conduction electrons. (b) A coupling of the itinerant spins with the MKC state and the gauge field. (c) Spin-polarized subbands of the free quasiparticles.

$$\varepsilon_{k-q_n/2, \sigma} = \varepsilon_{k+q_n/2, \sigma'} \quad (7)$$

The requirement condition is satisfied for special $k = k_n$ for a given n . In the spin-conserved scattering ($\sigma = \sigma'$), the energy conservation is satisfied for only $k_n = 0$ and the scattering term turns into zero [$\sin(ka) = 0$ in Eq. (5)] and has no effect on the quasiparticle spectrum.

The spin-flipping parts come from $A_q^\pm = \sum_{n=-\infty}^{\infty} A_n^\pm \delta_{q,nG}$, where the n th order reflection intensity is given by

$$A_n^\pm = \mp 2\Lambda \frac{n^2 e^{\mp n\gamma}}{\sinh(2n\gamma)}. \quad (8)$$

Here, $\Lambda = (\pi/\kappa K)^2 G_{\text{MKC}} a_0/2$ and $\gamma = \pi K'/K$. In the scheme of the reduced zone determined with respect to the superlattice BZ, $[-G_{\text{MKC}}/2, G_{\text{MKC}}/2]$, the condition given by Eq. (7) gives crossing points of the spin up and down bands. Then, it is expected that the umklapp scattering given by Eq. (5) lifts the accidental degeneracy and a resultant gap is formed due to Bragg reflection. A control of the G_{MKC} by a varying magnetic field enables to adjust the Fermi level to this gap region and move from metal to band insulator state.

In the reduced zone scheme, the gap at the crossing points $-k_n + nG_{\text{MKC}}/2$ is $\Delta_n^- = 4t|A_n^- \sin(k_n a)|$. On the other hand, the gap at the crossing points $k_n - nG_{\text{MKC}}/2$ is $\Delta_n^+ = 4t|A_n^+ \sin(k_n a)|$. This means that $\Delta_n^- \neq \Delta_n^+$ [see Fig. 2(a)]. This unusual asymmetry in the gap magnitudes is a direct consequence of chirality. That is to say, G_{MKC} and $-G_{\text{MKC}}$ are interchanged when we make change \mathbf{D} to $-\mathbf{D}$. So, the direction of \mathbf{D} directly comes up in the quasiparticle spectrum via the sd coupling. Note an analogy with an asymmetry of electron spectrum in materials with a toroidal state [18].

What is further interesting is an appearance of an oscillating spin structure in the electron subsystem for this band insulator state. Indeed, the crossing point in the reduced zone scheme corresponds to the states $|k - nG_{\text{MKC}}/2, \uparrow\rangle$ and $|k + nG_{\text{MKC}}/2, \downarrow\rangle$ in the extended scheme, which are evenly mixed by the Bragg reflection to give a new spin state, $|\varphi; \pm\rangle = (\pm e^{-inG_{\text{MKC}}(z-a)/2} |k, \uparrow\rangle + e^{inG_{\text{MKC}}z/2} |k, \downarrow\rangle) / \sqrt{2}$. By taking the expectation value of $s^{\bar{x}} = (|\uparrow\rangle\langle\downarrow| + |\downarrow\rangle\langle\uparrow|)/2$ and $s^{\bar{y}} = -i(|\uparrow\rangle\langle\downarrow| - |\downarrow\rangle\langle\uparrow|)/2$, we have the spin density $\langle\varphi; \pm|s^{\bar{x}}|\varphi; \pm\rangle = \pm \cos[nG_{\text{MKC}}(z-a)/2]$ and $\langle\varphi; \pm|s^{\bar{y}}|\varphi; \pm\rangle = \pm \sin[nG_{\text{MKC}}(z-a)/2]$. It is noted that this oscillating spin density wave is represented in the local frame corotating with the local spins. Therefore, in the crystal frame, this planar structure is further twisted in accordance with the MKC texture. This case of the primary reflection $n = 1$ is depicted in Figs. 2(b) and 2(c).

To confirm qualitative arguments given above, we present a microscopic calculation of resistivity under a steady current flowing state. For this purpose, we follow Zubarev's nonequilibrium density operator method, where a "dynamical molecular field," or else a response

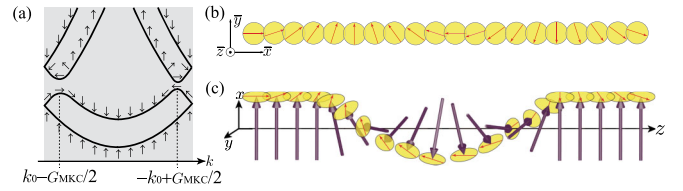


FIG. 2 (color online). (a) The gap opening at the crossing points of spin up and down bands. Spatial structures of the itinerant spins in the insulating state due to the primary reflection $n = 1$ are depicted in the local frame (b) corotating with the local spins and the crystal frame (c).

parameter, originating from a nonequilibrium background is introduced to determine a new density operator [19]. The field is conjugated to a basic dynamical variable, which is a main feature of the nonequilibrium state. In our treatment, this dynamical background is the dc current flowing state, and the current-density operator, $\mathcal{J} = -e \sum_{k, \sigma} v_k b_{k\sigma}^\dagger b_{k\sigma}$, constitutes the basic dynamical variable. Here, $e > 0$ is the elementary charge and $v_k = \hbar^{-1} \partial \varepsilon_{k, \sigma} / \partial k$ is the group velocity of the conduction electrons.

Using the approach, we extract the magnetic field dependence of the dc resistivity in the following form

$$\rho(H)/\rho_{\text{max}} = \mathcal{N}(H)/\mathcal{N}_{\text{max}}, \quad (9)$$

where $\mathcal{N}(H) = \lim_{\omega \rightarrow 0} \langle \dot{\mathcal{J}}; \dot{\mathcal{J}} \rangle_{\omega+i\varepsilon}$, ρ_{max} and \mathcal{N}_{max} are maximal values. The correlation function is defined by $\langle \dot{\mathcal{J}}; \dot{\mathcal{J}} \rangle_{\omega+i\varepsilon} = \int_0^\infty dt e^{i\omega t - \varepsilon t} \int_0^1 dx \langle \dot{\mathcal{J}}(t); \dot{\mathcal{J}}(i\beta\hbar x) \rangle_{\text{eq}}$. Here, the average $\langle \cdots \rangle_{\text{eq}} \equiv \text{Tr} \{ \rho_{\text{eq}} \cdots \}$, where $\rho_{\text{eq}} = \exp(-\beta \mathcal{H}_{\text{QP}}) / \text{Tr} \{ \exp(-\beta \mathcal{H}_{\text{QP}}) \}$ is the equilibrium density operator, and $\beta = 1/(k_B T)$. In contrast to Kubo's formula for a linear response of an isolated system, Eq. (9) gives a response of an open system that in contact with a heat bath.

The time derivative, $\dot{\mathcal{J}} = i\hbar^{-1} [\mathcal{H}, \mathcal{J}]$, is computed through the full Hamiltonian and reads as

$$\begin{aligned} \dot{\mathcal{J}} &= 2ie\hbar^{-1} \sum_{k, q} (v_{k+q/2} - v_{k-q/2}) e^{-iq a_0/2} \\ &\quad \times \sin(ka_0) \hat{b}_{k+q/2}^\dagger (A_q \cdot \boldsymbol{\sigma}) \hat{b}_{k-q/2}. \end{aligned} \quad (10)$$

After lengthy but straightforward computation, we obtain

$$\begin{aligned} \mathcal{N}(H) &= \sum_{k, n} \Gamma_n [v_k (v_{k+nG_{\text{MKC}}/2} - v_{k-nG_{\text{MKC}}/2})]^2 \\ &\quad \times f_{k+nG_{\text{MKC}}/2, \uparrow} (1 - f_{k+nG_{\text{MKC}}/2, \uparrow}) \\ &\quad \times \delta(\varepsilon_{k+nG_{\text{MKC}}/2, \uparrow} - \varepsilon_{k-nG_{\text{MKC}}/2, \downarrow}), \end{aligned} \quad (11)$$

where f is the Fermi-Dirac distribution function and n runs over nonzero integers. The total spin-flipping strength is given by

$$\Gamma_n = 2\pi\hbar e^2 \left(\frac{\pi n}{K\kappa} \right)^4 G_{\text{MKC}}^2 \frac{e^{2\pi n K'/K}}{\sinh^2(2\pi n K'/K)}. \quad (12)$$

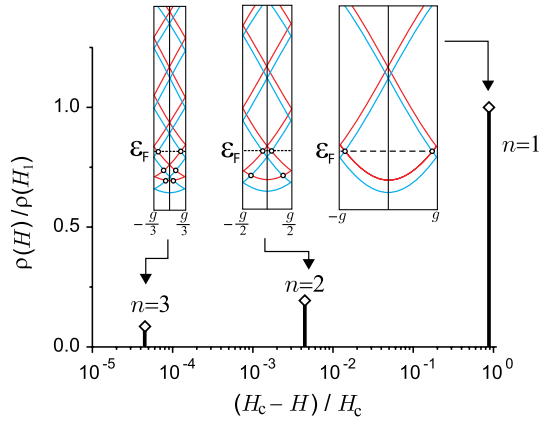


FIG. 3 (color online). Resonant resistivity at zero temperature. Here, $\rho_{\max} = \rho(H_1)$. The parameters are taken as $Q_0 = 10^2$, $h_{sd} = 9.85 \times 10^{-2}$, $t = 1$, and $n_c = 0.9$. The above panel shows an evolution of superlattice BZ with the magnetic field, where $g = G_{\text{MKC}}^{(1)}$.

In Fig. 3 the resonant zero-temperature resistivity is presented. In this case the peaks of the n th order intensities $\Gamma_n \cos^2[k_{F\uparrow}(n_c) - |n|G_{\text{MKC}}(H_n)/2]$ are observed at the magnetic fields H_n determined from the condition $\sin(k_{F\uparrow}(n_c) - |n|G_{\text{MKC}}/2) \sin(|n|G_{\text{MKC}}/2) = h_{sd}/(2t)$, where $k_{F\uparrow}(n_c)$ is Fermi momentum at given electron concentration per site, $0 < n_c < 2$. At the resonance value H_n , the superlattice BZ is n -fold reduced as compared with the $n = 1$ case, $G_{\text{MKC}}^{(1)}$, and the n -order points of an accidental Kramers degeneracy in the electron spectrum pass successively through the Fermi level. It is to be noted that in the phenomenological picture given in Fig. 2(a), degeneracy at the band crossing is lifted in a nonperturbative manner. Consequently, it is expected that the effective mass diverges at the top and the bottom of the bands. However, in the microscopic approach presented here, the degeneracy is not lifted and the degenerate perturbation gives the divergent mass at the crossing points. This is the reason why we have delta-function-like spikes of the resistivity in Fig. 3.

Finally, we discuss previous studies relevant to the present theory. The case of DW scattering was discussed in Ref. [20], where a gauge field created by local spins is a source of electron scattering. It is noted that their analysis is justified in a clean limit, or in a ballistic regime of electron transport. This issue has been previously addressed in Refs. [21] for a DW problem. However, in contrast to spatially localized domain walls, a resistivity due to Bragg scattering is a bulk effect. More importantly, the size of the superlattice is tunable by the magnetic field. We stress as well that an appearance of spin density wave in the electron subsystem for the band insulating state resembles an effect of spin accumulation due to a domain wall considered in Refs. [6]. This is, however, a secondary effect of the Bragg scattering, and not an independent source of the voltage drop as it has been postulated by Šimánek.

J.K. acknowledges a Grant-in-Aid for Scientific Research (A) (No. 22245023) from the Ministry of

Education, Culture, Sports, Science and Technology, Japan. A.S.O. and I.V.P. acknowledge Grant RFBR No. 10-02-00098-a.

- [1] A. Yamaguchi *et al.*, *Phys. Rev. Lett.* **92**, 077205 (2004); M. Kläui *et al.*, *Phys. Rev. Lett.* **94**, 106601 (2005); M. Yamanouchi *et al.*, *Phys. Rev. Lett.* **96**, 096601 (2006); L. Berger, *J. Appl. Phys.* **55**, 1954 (1984); S. Zhang and Z. Li, *Phys. Rev. Lett.* **93**, 127204 (2004); G. Tatara and H. Kohno, *Phys. Rev. Lett.* **92**, 086601 (2004).
- [2] L. Berger, *Phys. Rev. B* **33**, 1572 (1986); S. A. Yang *et al.*, *Phys. Rev. Lett.* **102**, 067201 (2009).
- [3] U. Ruediger *et al.*, *Phys. Rev. Lett.* **80**, 5639 (1998); U. Ebels *et al.*, *Phys. Rev. Lett.* **84**, 983 (2000); A. Aziz *et al.*, *Phys. Rev. Lett.* **97**, 206602 (2006); C. Hassel *et al.*, *Phys. Rev. Lett.* **97**, 226805 (2006).
- [4] P. M. Levy and S. Zhang, *Phys. Rev. Lett.* **79**, 5110 (1997); T. Taniguchi and H. Imamura, *Phys. Rev. B* **81**, 012405 (2010).
- [5] G. Tatara and H. Fukuyama, *Phys. Rev. Lett.* **78**, 3773 (1997).
- [6] E. Šimánek, *Phys. Rev. B* **63**, 224412 (2001); E. Šimánek and A. Rebei, *Phys. Rev. B* **71**, 172405 (2005); V. K. Dugaev, J. Barnaś, A. Łusakowski, and Ł. A. Turski, *Phys. Rev. B* **65**, 224419 (2002).
- [7] C. H. Wong and Y. Tserkovnyak, *Phys. Rev. B* **80**, 184411 (2009).
- [8] R. P. van Gorkom, A. Brataas, and G. E. W. Bauer, *Phys. Rev. Lett.* **83**, 4401 (1999); F. S. Bergeret, A. F. Volkov, and K. B. Efetov, *Phys. Rev. B* **66**, 184403 (2002); C. Wickles and W. Belzig, *Phys. Rev. B* **80**, 104435 (2009).
- [9] I. E. Dzyaloshinskii, *J. Phys. Chem. Solids* **4**, 241 (1958).
- [10] T. Moriya, *Phys. Rev.* **120**, 91 (1960).
- [11] I. E. Dzyaloshinskii, *Sov. Phys. JETP* **19**, 960 (1964); **20**, 665 (1965).
- [12] Yu. A. Izyumov, *Sov. Phys. Usp.* **27**, 845 (1984).
- [13] I. G. Bostrem, J. I. Kishine, and A. S. Ovchinnikov, *Phys. Rev. B* **77**, 132405 (2008); **78**, 064425 (2008); A. B. Borisov, J. I. Kishine, I. G. Bostrem, and A. S. Ovchinnikov, *Phys. Rev. B* **79**, 134436 (2009); I. G. Bostrem, J. Kishine, R. V. Lavrov, and A. S. Ovchinnikov, *Phys. Lett. A* **373**, 558 (2009).
- [14] J. I. Kishine and A. S. Ovchinnikov, *Phys. Rev. B* **79**, 220405(R) (2009).
- [15] J. I. Kishine, A. S. Ovchinnikov, and I. V. Proskurin, *Phys. Rev. B* **82**, 064407 (2010).
- [16] J. Kishine, K. Inoue, and Y. Yoshida, *Prog. Theor. Phys. Suppl.* **159**, 82 (2005); B. Roessli *et al.*, *Phys. Rev. Lett.* **86**, 1885 (2001).
- [17] Y. Kousaka *et al.*, *Nucl. Instrum. Methods Phys. Res., Sect. A* **600**, 250 (2009).
- [18] Yu. V. Kopaev, *Phys. Usp.* **52**, 1111 (2009).
- [19] D. N. Zubarev, V. G. Morozov, and G. Roepke, *Statistical Mechanics of Nonequilibrium Processes: Basic Concepts, Kinetic Theory* (Akademie Verlag, Berlin, 1996), Vol. 1.
- [20] A. Brataas, G. Tatara, and G. E. W. Bauer, *Phys. Rev. B* **60**, 3406 (1999).
- [21] J. Kishine, A. S. Ovchinnikov, and I. V. Proskurin, *J. Phys. Conf. Ser.* **286**, 012017 (2011).